

Performance Evaluation of Differential Geometry based Techniques for MRI Image Segmentation

Muhammad Amir Khan, Jawad Haider Kazmi, Kalim Qureshi, Laiq Khan

Department of Electrical Engineering CIIT Abbottabad, Pakistan
Department of Computer Science CIIT Abbottabad, Pakistan
Department of Information Science Kuwait University, Kuwait
Department of Electrical Engineering CIIT Abbottabad, Pakistan

Abstract: Image Segmentation plays a crucial role in many medical-imaging applications by automating or facilitating the delineation of anatomical structures and other regions of interest. There are different categories of Image segmentation techniques having sub-category of some methods. Like pattern recognition techniques, model based approaches, tracking-based approaches, neural network based approaches etc. We implement three differential geometry based vessel extraction techniques, and compare the performance evaluation against Pratt's FOM, and found an optimum technique among them.

Key words: Image Segmentation, Thinnetworks, Multi-scale, Anisotropic diffusion, Figure of merit.

INTRODUCTION

Image segmentation plays a crucial role in many medical-imaging applications by automating or facilitating the delineation of anatomical structures and other regions of interest. Image segmentation is the method in which the inputs are images, but the outputs are attributes extracted from those images. Segmentation subdivides an image into its constituent regions or objects. In general image segmentation based on one of two basic properties of intensities values: discontinuity and similarity. In first category, the approach is to partition an image based on abrupt changes in intensity such as edges in an image while second category is based on partitioning an image into regions that are similar according to a set of predefined criteria (Gonzalez and Woods, 2001). Edge detection approach is the most common for detecting meaningful discontinuous in gray level. Medical images are used in diagnosis as well as in study of basic human physiology and anatomy. These images give valuable insights of the human body without tearing it. There are multitude of modalities including digital radiography, computed tomography, magnetic resonance imaging, positron emission tomography, single photon emission computed tomography and ultrasonography, for obtaining these image in either two or three dimensions. Three dimensional (3D) images provide both qualitative and quantitative information about a target organ (Huiguang *et al.*, 2006). Our focus on MRI images because it is a rapidly emerging technique that provides high quality images and potentially provides much more diagnostic information than do conventional imaging modalities. Magnetic resonance angiography (MRA) is a variation of MRI in with blood flow in the vessel is imaged. Image segmentation algorithms are the key components of automated radiological diagnosis systems. There are different categories of image segmentation techniques having sub-category of some methods. Like Pattern recognition techniques, Model based approaches, Tracking-based approaches, Neural Network based approaches etc (Cemil Kirbas and Francis Quek, 2004). We worked on Differential Geometry technique which lie under the pattern recognition techniques. Differential Geometry (DG) based method treats images as hyper-surfaces and extracts features using the curvature and the crest lines of the surface. The crest points of the hyper-surface correspond to the center lines of the vessel structure. The 2D and 3D images are treated similarly. In DG surface can be described by two principal curvatures and their corresponding orthogonal directions, called principal directions. The principal curvature corresponds to the eigenvalues of the Weingarten matrix and the principal directions are eigenvectors. Crest points, which are the intrinsic properties of the surfaces, are the local maxima of the maximum curvature on the hyper-surface. Crest lines are intuitively the most salient features of the surface. Center-lines are obtained by linking the crest-points (Prinet *et al.*, 1996). We have implemented three DG algorithms and have compared the performance of edges detected using Pratt's Figure of Merit.

Corresponding Author: Muhammad Amir Khan, Department of Electrical Engineering CIIT Abbottabad, Pakistan

Differential Geometry:

Differential Geometer is a branch of Geometry. A through introduction to the Differential Geometry can be found in Docarmo (Manfredo Do Carmo, 2000) and Koenderink (2001). Here, we only present a short introduction to the implementation of DG to the surfaces (Monga and Benayoun, 1992). Let $I(x,y,z)$ be the grey level function of a 3D image and let M is an application from

an upset $U \subset \mathfrak{R}^3$ to E defined as:

$$M : (x,y,z) \rightarrow (x,y,z,I(u,v,w)) \tag{1}$$

The parametric surface traced by the image is given by

$$\Sigma = \{\vec{v} \in \mathfrak{R}^4 / \vec{v} = (x, y, z, I(u, v, w))\}, \tag{2}$$

Where $u = x, v = y, w = z$ and I is the grey level function of the 3D image.

The tangent plan to the surface at a point P_0 with coordinates (x_0, y_0, z_0, I_0) , is defined by:

$$(\vec{M}_u, \vec{M}_v, \vec{M}_w), \text{ with } \vec{M}_u = \delta \vec{M} / \delta u |_{P_0}, \vec{M}_v = \delta \vec{M} / \delta v |_{P_0} \text{ and } \vec{M}_w = \delta \vec{M} / \delta w |_{P_0}. \tag{3}$$

The rest of the paper is organized as follows. In Section 2, we present the selected algorithms/techniques for the study and their working. Section 3 provides the detailed description of the experiment results, tools used and methodology to evaluate the performance of the selected algorithms/techniques. A detailed discussion on the results is also included in this section. Finally, in Section 4 we gave the conclusions and future directions of this work.

Methodology:

For this study, we have selected three popular DG based algorithms/techniques. We now will present a brief introduction and working of each of these techniques.

Thin-networking Extraction:

Thin network extraction has the major importance in medical vascular imaging for diagnostic, therapy planning and surgery. The mathematical formulae used to compute the curvature and directions are presented in (Monga and Benayoun, 1992). They require the preliminary calculation of the first and second order partial derivatives. We can easily notice that the hyper-surface, obtain three curvature. It appears that the curvatures whose amplitude is maximal (the maximum curvature) is related to the radius of the vessels and is of great interest to extract features, such as thinnest from the images. Crest lines are obtained by using comparison procedure: a point P on the surface is a crest point, if its two nearest neighbors taken along the principal direction have a maximum curvature whose amplitude is lower than point P . The result shows that this point will be localized on the axis of the vessel. Linked together, crest points form the center-lines. This approach has two major interests: first it require no priori knowledge and it is entirely automatic, without any need of user interaction.

The algorithm is outlined here:

1. Compute the partial derivative of the image in x and y up to order two.

This can be written as:

$$f_0(x) = c_0(1 + \alpha|x|)^{e^{-\alpha|x|}}, \text{ (smoothing operator);}$$

$$f_1(x) = -c_1x\alpha^2e^{-\alpha|x|}, \text{ (first derivative operator)}$$

$$f_2(x) = c_2(1 - c_3\alpha|x|)e^{-\alpha|x|}, \text{ (second derivative operator).}$$

2. Compute the principal curvatures and directions (both these values corresponds to the eigen values and eigen vectors, respectively) at each voxel on the image.
3. For each voxel P (with maximum curvature and direction called c_1 and d_1 respectively), compute the maximum curvature c_1^a and c_1^b at points P_a and P_b , located along d_1 at a unit distance from P .

Multi-scale Approach:

As discussed in Section 2.1, for a simple data, we can obtain good results using a single value for α , and for more complex data the suitable value for α varies depending on the area of the 3D image, for noisy data only the crest lines that can be seen using different scale define reliable features. Therefore similar to the edge detection (Jean Ponce and Michael Brady, 2005) and to the crest line extraction in depth maps (Monga *et al.*, 1994), it is of great interest to use a multi-scale approach. One such algorithm, used in our study is outlined here, obtains the results at different scales α_i for $i=1,2,3,\dots,n$. It then merges these result using an Adjacency Graph $G_{\alpha_1, \alpha_2, \alpha_3, \dots, \alpha_n}$.

Adjacency Graph $G_{\alpha_1, \alpha_2, \alpha_3, \dots, \alpha_n}$ is a valuated graph built as follows:

1. Each node of $G_{\alpha_1, \alpha_2, \alpha_3, \dots, \alpha_n}$ is attached to a point (i, j, k) such that for at least one scale α_m , we have $Z_{\alpha_m}(i, j, k) = 1$. The features attached to each node are:
 - a. the coordinates of the corresponding 3D point (i, j, k)
 - b. the value of the scales for which point is a crest point all the α_p such that $Z_{\alpha_p}(i, j, k) = 1$
 - c. the differential characteristics extracted for all the scales (principal curvatures and principal curvatures directions, value of the extremity criterion).
2. An edge joining two nodes of $G_{\alpha_1, \alpha_2, \alpha_3, \dots, \alpha_n}$ if and only if the tow corresponding points are adjacent for the 26-connectivity. Therefore $G_{\alpha_1, \alpha_2, \alpha_3, \dots, \alpha_n}$ represents the results of the crest points extraction for the different scales and their spatial relationships.

The above algorithm can be stated in simples terms as:

1. Computation of a zero-crossing of the extremity criterion for a given set of scales $\alpha_1, \alpha_2, \alpha_3, \dots, \alpha_n$; the result is a set of images $Z_{\alpha_1}, Z_{\alpha_2}, Z_{\alpha_3}, \dots, Z_{\alpha_n}$
2. Building of the multi-scale graph $G_{\alpha_1, \alpha_2, \alpha_3, \dots, \alpha_n}$
3. Pruning of $G_{\alpha_1, \alpha_2, \alpha_3, \dots, \alpha_n}$ to select reliable crest points.

Anisotropic Diffusion:

Is a technique for the extraction of features from images. This process can be applied in medical image analysis to segment the different anatomical structures. The method is based on the explicit weighting of the diffusion in the directions of the gradient, and minimum and maximum curvatures.

The algorithm is stated as:

Let

1. e_1 and e_2 be the two vectors in the principal directions of the curvature of the plane orthogonal to the gradient of the intensity of the
2. e_1 will be a unit vector in the direction of the maximum curvature k_1
3. similarly, e_2 will be a unit vector in the direction of the minimum curvature k_2

Performance Evaluation Metrics:

Performance evaluation for the image processing techniques can be done subjectively and objectively. However, for many computer imaging applications the subjective measures tend to be the most useful. For the objective analysis, we have selected Prett’s Figure of Merit (FOM) (Jean-Philippe Thiron and Alexis Gourdon, 1995).

FOM is defined as:

$$FOM = 1 / I_N \sum_{i=1}^{I_F} 1 / (1 + \alpha d_i^2) \tag{4}$$

Where

I_N = the maximum of I_I and I_F

I_I = the number of ideal edge points in the image

I_F = the number of edge points found by the edge detector

α = a scaling constant that can be adjusted to adjust the penalty for offset edges

d_i = the distance of a found edge point to an ideal edge point.

Euclidean distance, based on actual physical distance:

$$d = [(r_1 - r_2)^2 + (c_1 - c_2)^2]^{1/2} \tag{5}$$

For this metric, FOM will be 1 for a perfect edge and this metric assigns a better rating to smeared edges than to offset or missing edges.

Pratt considered the three types of errors which are: (1) missing valid edge points, (2) classifying noise pulses as valid edge points, and (3) smearing of edges. If these errors do not occur, we can say that we have achieved success. Figure 1 shows these three types of errors described above.

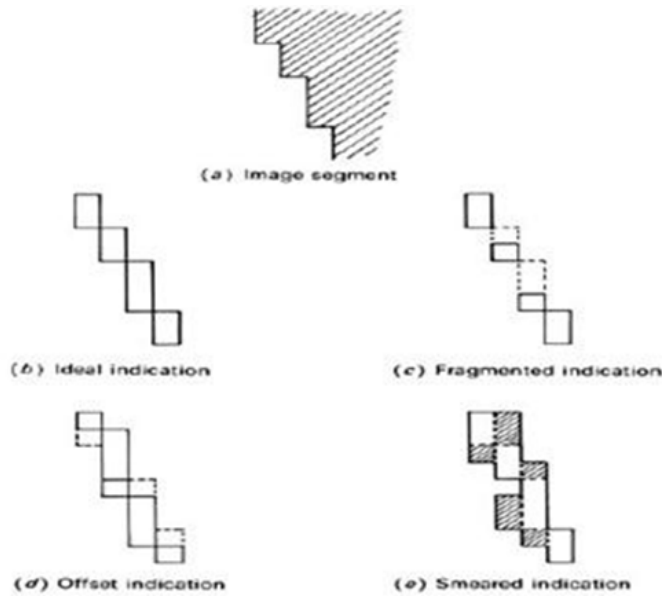


Fig. 1: Errors which can be detected by FOM

RESULTS AND DISCUSSION

We now present the results of applying the techniques described in Section 2 on MRI images. All these algorithms are applied slice-by-slice on 3 different MRI datasets, as described in Table 1.

Table 1: Datasets used in the experiment

Name	Dimensions
Data Set 1	512 x 64 x 512
Data Set 2	256 x 128 x 128
Data Set 3	256 x 256 x 128

Figure 2,3,4 and 5, shows the working of Thinnetwork extraction techniques discussed in Section 2.1.



Fig. 2: Input Slice 1 of MRI Image



Fig. 3: Output Slice 1 of MRI Image



Fig. 4: Input Slice 2 of MRI Image

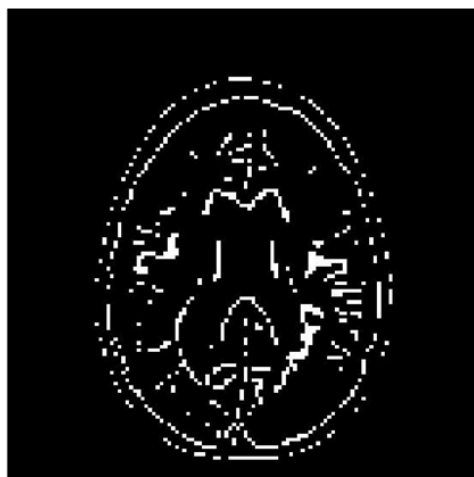


Fig. 5: Output Slice 2 of MRI Image

Figure 6, 7, 8 and 9 show the working of Multiscale algorithm discussed in Section 2.2.

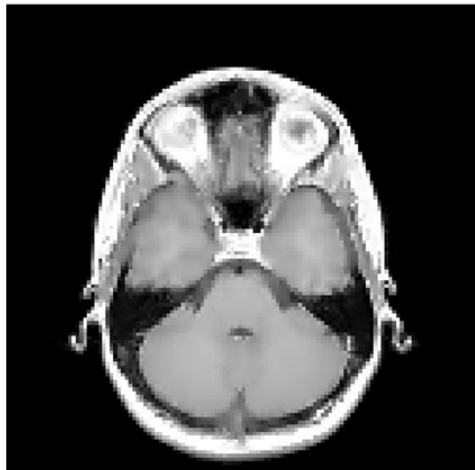


Fig. 6: Input Slice 1 of MRI Image

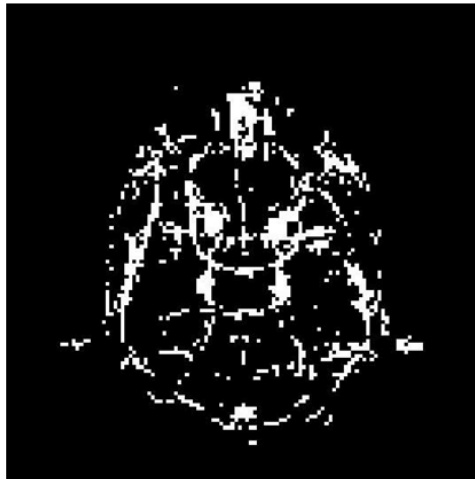


Fig. 7: Output Slice 1 of MRI Image



Fig. 8: Input Slice 2 of MRI Image



Fig. 9: Output Slice 2 of MRI Image

Figure 10, 11, 12 and 13 show the working of Anisotropic Diffusion algorithm discussed in Section 2.3.

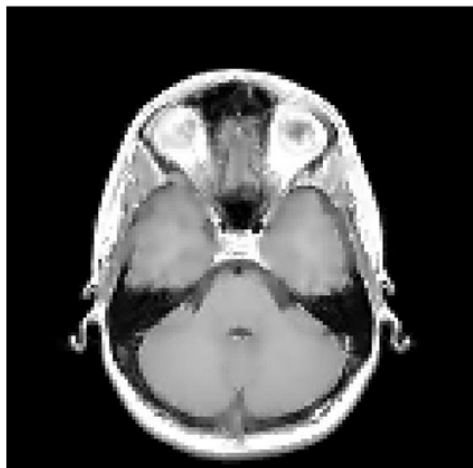


Fig. 10: Input Slice 1 of MRI Image

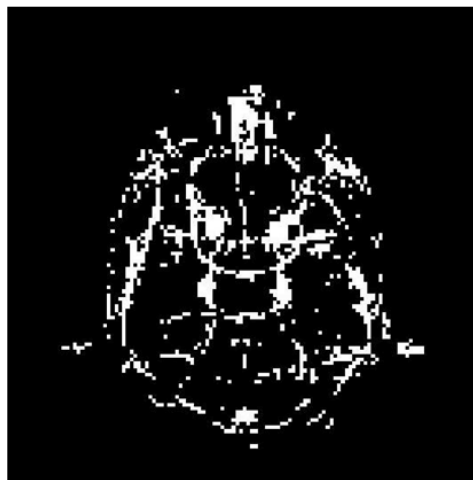


Fig. 11: Output Slice 1 of MRI Image



Fig. 12: Input Slice 2 of MRI Image



Fig. 13: Output Slice 2 of MRI Image

After testing the performance of the Differential Geometry algorithm on simple images thinnetworks techniques gave acceptable results because on simple images contain no noise or bit noise added during acquisition, Multiscale technique works on different sigma value its results will be better when complex and noisy images used for testing, as far as the simple images are concerned results shows low values, because scale used for the experiment is higher. But anisotropic diffusion gave best results because of its smoothing technique and it also work well on complex and noisy images.

We have further tested these techniques/algorithms for FOM. Since, MRI images are very complex and finding the exact amount of edges is difficult, so, we have used some synthetic image and have applied these algorithm on them. The results of these and the calculated FOM is presented here.

Figure 14 shows the two synthetic images, with known edges, used in this experiment, while 15, 16 and 17 shows, respectively, the output images when Thinnetwork, Multiscale and Anisotropic Diffusion algorithm are applied.

Table 2: Datasets used in the experiment

Input Image	TN	MS	AN
1	0.63	0.70	0.75
2	0.65	0.68	0.73



Fig. 14: Two synthetic images used for FOM

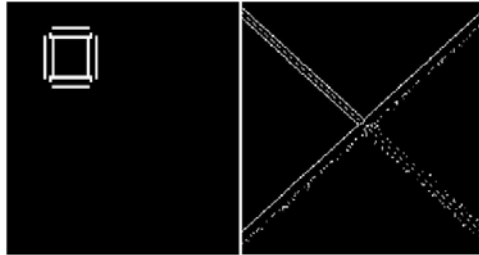


Fig. 15: Output synthetic images when TN is applied

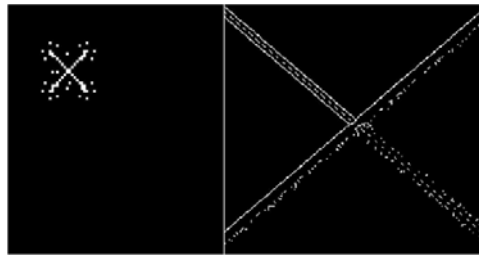


Fig. 16: Output synthetic images when MS is applied

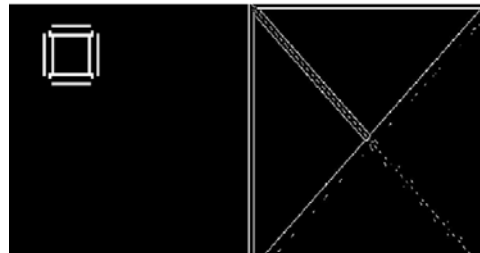


Fig. 17: Output synthetic images when AN is applied

Table 2: Shows the FOM calculation for the three algorithm using the equation (4).

$$FOM = 1/I_N \sum_{i=1}^{I_F} 1/I + \alpha d^2$$

Conclusion and Future Work:

This work presented a comparative study of three selected differential geometry based MRI vessel extraction techniques/algorithms. From this study we can conclude that vessel extraction is a complex task and one technique alone is not sufficient for the accomplishment of the task. In future we plane to develop hybrid technique/algorithms for better results.

REFERENCES

- Cemil Kirbas and Francis Quek, 2004. A review of vessel extraction techniques and algorithms. *ACM Comput. Surv.*, 36(2): 81–121.
- Jean Ponce and Michael Brady, 2005. Toward a surface prima 1 sketch. *In Proceedings, IJCAI*,
- Jean-Philippe Thirion and Alexis Gourdon, 1995. Computing the differential characteristics of iso-intensity surface. *Comput. Vis. Image Underst.*, 61(2): 190–202.
- Huiguang, He, Jie Tian, Mingchang Zhao, Jian Xue and Ke Lu, 2006. 3d medical imaging computation and analysis platform. *Industrial Technology, 2006. ICIT 2006. IEEE International Conference on*, pages 1160–1165.
- Koenderink, J.J., 2001. *Solid shapes*. MIT Press.
- Manfredo Do Carmo. *Differential Geometry of Curves and Surfaces*. Prentice-Hall, Englewood Cliffs, 2000.
- Gonzalez, R.C. and R.E. Woods, 2001. *Digital Image Processing*. Addison-Wesley Longman Publishing Co., Inc., 2nd edition.
- Monga, O. and S. Benayoun, 1992. Using partial derivatives of 3d images to extract typical surface features. *AI, Simulation and Planning in High Autonomy Systems, 1992. Integrating Perception, Planning and Action., Proceedings of the Third Annual Conference of*, 225–236.
- Monga, O., R. Lengagne and R. Deriche, 1994. Crest lines extraction in volume 3d medical images: a multi-scale approach. *Pattern Recognition, Conference A: Computer Vision and Image Processing., Proceedings of the 12th IAPR International Conference on*, 1: 553–555.
- Prinet, V.O. Monga, C. Ge, S.L. Xie and S.D. Ma, 1996. Thin network extraction in 3d images: application to medical angiograms. *Pattern Recognition, 1996., Proceedings of the 13th International Conference on*, 3: 386–390.